Modelling, Measurement and Control B
Vol. 87, No. 2, June, 2018, pp. 68-77
Journal homepage: http://iieta.org/Journals/MMC/MMC_B

A hybrid intelligent model for crack diagnosis in a free-free aluminium beam structure

Sanjay K. Behera[1*], Dayal R. Parhi[2], Harish C. Das[3]

[1] Mechanical Engineering Department, Siksha 'O' Anusandhan Deemed to be University, Bhubaneswar, Odisha 751030, India
[2] Robotics Laboratory, Mechanical Engineering Department, National Institute of Technology, Rourkela, Odisha 769008, India
[3] Mechanical Engineering Department, National Institute of Technology, Shillong, Meghalaya 793003, India

Corresponding Author Email: sanjaybeheraoec@gmail.com

https://doi.org/10.18280/mmc_b.870202

Received: 3 April 2018
Accepted: 17 June 2018

Keywords:
crack, fuzzy logic, genetic algorithm, natural frequency, rule base

ABSTRACT

In a damaged beam structure, vibration characteristics like natural frequencies and mode shapes undergoes a sharp change due to presence of cracks. In the current investigation, a hybrid intelligent model has been proposed for detection of crack in an aluminium beam structure with free-free boundary conditions. A theoretical investigation has been carried out initially to mathematically model the vibrational parameters of a beam structure. The theoretical model is also supported by an experimental investigation using a free-free aluminum beam of specified dimension in presence and absence of crack. The impact of variations in crack depths and crack locations on natural frequency and mode shapes have been studied extensively. The hybrid intelligent model consisted of Fuzzy logic, Genetic algorithm and Rule based technique in different combinations. Relative natural frequencies of the beam structure are fed as inputs to the hybrid model, and relative crack depth and crack locations are generated as the outputs. Finally, the paper also gives an insight into the comparison of vibrational parameters obtained from numerical and experimental result with that of the proposed hybrid intelligent model.

1. INTRODUCTION

Maintaining structural integrity is highly essential in beam structures as cracks are one of the internal damage within the beam structure and its early detection can prevent further degeneration. The presence or development of crack in a structure subjected to dynamic vibration is detrimental to the entire system and may lead to decrease in life expectancy of the system. Crack detection and diagnosis of a structure based on the changes in its vibration parameters under a dynamic vibration condition have been the major area of research since last few decades. In the present study, efforts have been made to diagnose the presence of crack in a free-free aluminium beam based on hybrid intelligent concept. A proper fault diagnosis of beams, structures or machine components to improve service life is essential [1-2]. Various non-destructive techniques are in place to solve the above mentioned problem, but they have not been proved to be cost effective. The vibration based methodologies are the effective way for such diagnosis. Artificial Intelligence technique uses all modal parameters like relative natural frequency, relative mode shapes as input parameters applied to the technique for crack diagnosis. An effort in this direction has been made to develop a hybrid intelligence based model to automate an effective damage diagnosis of a cracked beam structures. The proposed model has been trained by feeding experimental and numerical data (initial data pool) under healthy and faulty structural condition separately. Some of the prominent researches in the area of damage detection can be summarized over here.

Ganguli [3] has used a fuzzy logic model based structural damaged detection technique of decreased stiffness at the damaged site specifically developed for diagnosis of blade rotor of a helicopter. Sazonov et al. [4] have presented a fuzzy logic based damage detection model employing the concept of finite element methodology for a simple beam structure. Pawar and Ganguli [5] have investigated the modal characteristics like changes in natural frequencies due to structural damage and modeled it for a cantilever beam with crack using finite element method and also formulated a genetic-fuzzy hybrid technique to locate the crack and estimate the crack size effectively. Chandrashekhar and Ganguli [6] have presented a novel concept by exploring a relationship between the changes in material properties and corresponding variations in vibration parameters (frequency) and used a fuzzy based model with a defuzzifier for damage diagnosis. Parhi and Kumar [7] have reviewed different methodologies available like energy methods, fuzzy logic, neural network methods, neuro-fuzzy hybrid technique, genetic algorithm, finite element analysis for crack diagnosis. He et al. [8] have proposed a model based on genetic algorithm concept to detect cracks on a shaft and optimized it using finite element methods. Hao and Xia [9] have used a real number encoding system in the genetic algorithm for identification of cracks in the damaged structures and compared the changes in measurements using minimized objective function for the structure before damage and after damage. Krawczuk [10] have established a work for damage diagnosis using a hybrid approach of wave propagation, genetic algorithm, and gradient technique in a beam structure. He and Hwang [11] have combined adaptive real-parameter genetic algorithm and simulated annealing to develop a suitable and effective algorithm for crack detection in a damaged beam structure. Perera and Torres [12] have formulated a non-classical optimization procedure using genetic algorithm and used it to identify damaged area in a structural beam element. Panigrahi et al. [13] have presented a paper on microscopic structural damage identification by formulating an objective function using AI technique based on genetic algorithm coupled with residual force methodology. Pawar and Ganguli [14] have used a composite matrix cracking model to apply on a thin walled hollow circular cantilever beam using stiffness approach. They carried out a study on changes in natural frequencies in a cracking model using a genetic fuzzy hybrid concept. The effectiveness of combined system is drawn through uncertainty representation of characteristics of fuzzy logic with leaning potential of genetic algorithm. Wu [15] has devised a fuzzy based system for automatic crack diagnosis in a car manufacturing unit. They have used fuzzy membership functions for representing input and output data and have presented that for necessary optimization of the data. Lo et al. [16] have developed an artificial intelligent technique on combined genetic-fuzzy algorithm for automatic fault diagnosis on Heating, ventilation, and air conditioning (HVAC) system. Suh et al. [17] have developed a technique to predict the crack position and depth of crack on a beam structure by employing a hybrid neuro- genetic combination technique. Saridakis et al. [18] studied the dynamic behavior of a shaft with two transverse cracks considered at any arbitrary positions at some distance from the clamped end. They developed a fuzzy logic based crack diagnosis model by using the effect of bending vibration of the cracked shaft. Kolodziejczyk et al. [19] have investigated the potential of various artificial intelligence techniques to predict the damage parameters due to dynamic contact systems. The proposed technique was designed and developed using fuzzy logic, neural network and genetic algorithm. The result from the developed hybrid methodology were in proximate to the experimental data.

From the extensive literature survey, it can be inferred that application of hybrid methodologies for crack detection in damaged structures have been rarely reported. Hybrid intelligent system is a software based diagnostic system that employs, in parallel, a combination of various methods and techniques from artificial intelligence subfields. In the present study, a combination of knowledge based expert systems with other artificial intelligent methods are considered that add more effectiveness to the diagnostic task. Here, efforts have been made to combine fuzzy logic with genetic algorithm and rule based methodology for the crack detection purpose. The relative natural frequencies of the damaged beam structure are fed as inputs to the hybrid system, and relative crack location and crack depth are generated as outputs of the system. The proposed hybrid intelligent model is also compared against the numerical and experimental results, and a good agreement has been observed.

2. THEORETICAL OVERVIEW FOR THE DETERMINATION OF VIBRATION CHARACTERISTICS OF THE CRACKED FREE-FREE BEAM

An analysis of a free-free beam having a transverse crack subjected to both bending and axial load has been considered in the present study. The stiffness matrix in presence of crack is derived as the inverse of compliance matrix. The equivalent compliance matrix is derived assuming cracked node as a cracked element having no length and mass.

Let U_i = additional displacement due to bending load and axial load, V_t = strain energy due to the crack

$$U_i = \frac{\partial V_t}{\partial P_i} \tag{1}$$

where V_t can be expressed as:

$$V_t = \int_0^{a_1} \frac{\partial V_t}{\partial a} da = \int_0^{a_1} J(a) da \tag{2}$$

where $J = \frac{\partial V_t}{\partial a}$ is strain energy release rate and a_1 is crack depth.

By the Pari's equation, the additional displacement can be expressed as:

$$U_i = \frac{\partial}{\partial P_i}\left[\int_0^{a_1} J(a) da\right] \tag{3}$$

The components of local flexibility matrix per unit width can be expressed as:

$$\alpha_{ij} = \frac{\partial U_i}{\partial P_j} = \frac{\partial^2}{\partial P_i \partial P_j}\int_0^{a_1} J(a)\, da \tag{4}$$

The final resulting flexibility matrix $\left[\alpha_{ij}\right]$ over the total breadth B for the beam with edge crack can be written as:

$$\left[\alpha_{ij}\right] = \frac{\partial U_i}{\partial P_j} = \frac{\partial^2}{\partial P_i \partial P_j}\int_{-B/2}^{+B/2}\int_0^{a_1} J(a) da dz \tag{5}$$

As per Tada et al. [20], the expression for strain energy release rate at crack location is written as:

$$J = \frac{1-v_1^2}{E}(\mathrm{K}_{11}+\mathrm{K}_{12})^2 \tag{6}$$

$$\frac{1}{E'} = \frac{1-v_1^2}{E} \quad \text{(plane strain)}$$

$$\frac{1}{E'} = \frac{1}{E} \quad \text{(plane stress)}$$

where K_{11} and K_{12} represent the stress intensity factors for mode I (opening of the crack) subjected under the load P_1 and P_2 defined as axial and bending load respectively.

Mathematically the stress intensity factors can be mathematically written in the form as below;

$$K_{ij} = \sigma_i \sqrt{\pi a}\left(F_i\left(\frac{a}{W}\right)\right) \tag{7}$$

where σ_i is stress at the crack cross section due to axial and bending load, so,

$$K_{11}=\frac{P_1}{BW}\sqrt{\pi a}\left(F_1\left(\frac{a}{W}\right)\right),\ K_{12}=\frac{6P_2}{BW^2}\sqrt{\pi a}\left(F_2\left(\frac{a}{W}\right)\right)$$

where terms F_1 and F_2 can be expressed as:

$$F_1\left(\frac{a}{W}\right)=\left\{\frac{2W}{\pi a}\tan\left(\frac{\pi a}{2W}\right)\right\}^{0.5}\times \left\{\frac{0.752+2.02(a/W)+0.37(1-\sin\left(\frac{\pi a}{2W}\right)^3}{\cos(\pi a/2W)}\right\} \tag{8}$$

$$F_2\left(\frac{a}{W}\right),=\left\{\frac{2W}{\pi a}\tan\left(\frac{\pi a}{2W}\right)\right\}^{0.5}\times \left\{\frac{0.923+0.191(1-\sin\left(\frac{\pi a}{2W}\right)^4}{\cos(\pi a/2W)}\right\} \tag{9}$$

Using equation (6) for strain energy release rate and putting it in equation (4), the flexibility matrix can be written as:

$$\alpha_{ij}=\frac{B}{E'}\frac{\partial^2}{\partial P_i\partial P_j}\int_0^{a_1}\left(K_{11}+K_{12}\right)^2 da \tag{10}$$

Taking $\varphi=(a/W)$, then $d\varphi=\dfrac{da}{W}$

We obtain $da=Wd\varphi$ and when, $a=0,\varphi=0$ $a=a_1,\ \varphi=a_1/W=\varphi_1$

From the relations above, the equation (10) becomes,

$$\alpha_{ij}=\frac{BW}{E'}\frac{\partial^2}{\partial P_i\partial P_j}\int_0^{\varphi_1}\left(K_{11}+K_{12}\right)^2 d\varphi \tag{11}$$

From the equation (10), calculating $\alpha_{11},\alpha_{12}(=\alpha_{21})$ and α_{22} we get:

$$\alpha_{11}=\frac{BW}{E'}\int_0^{\varphi_1}\frac{\pi a}{B^2W^2}2(F_1(\varphi_1))^2 d\varphi=\frac{2\pi}{BE'}\int_0^{\varphi_1}(\varphi_1)(F_1(\varphi_1))^2 d(\varphi_1) \tag{12}$$

$$\alpha_{12}=\alpha_{21}=\frac{12\pi}{E'BW}\int_0^{\varphi_1}(\varphi_1)F_1(\varphi_1)F_2(\varphi_1)d(\varphi_1) \tag{13}$$

$$\alpha_{22}=\frac{72\pi}{E'BW^2}\int_0^{\varphi_1}F_2(\varphi_1)F_2(\varphi_1)\,d(\varphi_1) \tag{14}$$

The inversion of compliance matrix give rise to a local stiffness matrix, i.e.

$$K=\begin{bmatrix}K_{11} & K_{12}\\ K_{21} & K_{22}\end{bmatrix}=\begin{bmatrix}\alpha_{11} & \alpha_{12}\\ \alpha_{21} & \alpha_{22}\end{bmatrix}^{-1}$$

Figure 1 shows a beam model and Figure 2 shows the geometry of beam with width=B, length=L, depth=W and depth of crack =a_1 positioned at distance L_1 from the left end with amplitudes in longitudinal vibration for the sections as $U_1(x, t)$ and $U_2(x, t)$ and the amplitudes of vibration under the application to bending at the sections as $Y_1(x, t)$ and $Y_2(x, t)$.

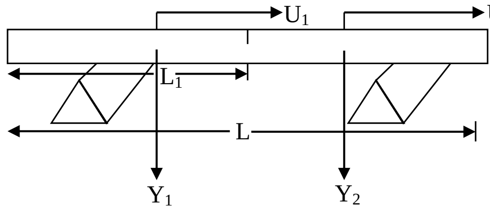

Figure 1. Beam model

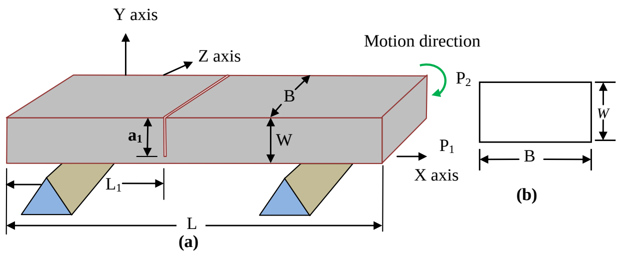

Figure 2. Geometry of beam, (a) free-free beam (b) Cross-sectional view of the beam

The normal functions of the system can be defined as:

$$\bar{U}_1=A_1cos(\bar{K}_u\bar{x})+A_2sin(\bar{K}_u\bar{x}) \tag{15a}$$

$$\bar{U}_2=A_3cos(\bar{K}_u\bar{x})+A_4sin(\bar{K}_u\bar{x}) \tag{15b}$$

$$\bar{Y}_1(\bar{x})=A_5cosh(\bar{K}_y\bar{x})+A_6sinh(\bar{K}_y\bar{x})+A_7cos(\bar{K}_y\bar{x})+A_8sin(\bar{K}_y\bar{x}) \tag{15c}$$

$$\bar{Y}_2(\bar{x})=A_9cosh(\bar{K}_y\bar{x})+A_{10}sinh(\bar{K}_y\bar{x})+A_{11}cos(\bar{K}_y\bar{x})+A_{12}sin(\bar{K}_y\bar{x}) \tag{15d}$$

where $\bar{U}=\dfrac{U}{L},\bar{X}=\dfrac{X}{L},\bar{Y}=\dfrac{Y}{L},\gamma=\dfrac{L_1}{L}$

$$\bar{K}_u = \frac{\omega L}{C_u}, \bar{K}_y = \left(\frac{\omega L^2}{C_y}\right)^{1/2}, C_u = \left(\frac{E}{\rho}\right)^{1/2},$$

$$C_y = \left(\frac{EI}{\mu}\right)^{1/2}, \mu = A\rho$$

A_i *(i=1, 12)* are constants, and their values can be calculated using boundary conditions. Following are the boundary conditions of the free-free beam under study are:

$$\bar{U}_1'(0)=0;\ \bar{Y}_1''(0)=0; \bar{Y}_1'''(0)=0;$$
$$\bar{U}_2'(1)=0;\ \bar{Y}_2''(1)=0;\ \bar{Y}_2'''(1)=0;$$

At the cracked location:

$$\bar{U}_1(\gamma)=\bar{U}_2'(\gamma);\ \bar{Y}_1(\gamma)=\bar{Y}_2(\gamma);$$
$$\bar{Y}_1'(\gamma)=\bar{Y}_2''(\gamma);\ \bar{Y}_1''(\gamma)=\bar{Y}_2'''(\gamma)$$
$$\bar{U}_2'(\gamma)=\bar{U}_3'(\gamma);\ \bar{Y}_2(\gamma)=\bar{Y}_3(\gamma);$$
$$\bar{Y}_2''(\gamma)=\bar{Y}_3''(\gamma);\ \bar{Y}_2'''(\gamma)=\bar{Y}_3'''(\gamma)$$

Also at the section of the crack, i.e. at distance L_1, due to absence of axial displacement on both left and right side of the crack, we have:

$$AE\frac{dU_1(L_1)}{dX} = K_{11}(U_2(L_1)-U_1(L_1))+$$
$$K_{12}\left(\frac{dY_2(L_1)}{dX}-\frac{dY_1(L_1)}{dX}\right)$$

Multiplying, the term $\frac{AE}{LK_{11}K_{12}}$ on both sides of the above expression, we get

$$M_1 M_2 \overline{U'}(\gamma) = M_2\bar{U}_2(\gamma)+M_1\bar{Y}_2'(\gamma)-M_1\bar{Y}_1'(\gamma)$$

where

$$M_1 = \frac{AE}{LK_{11}}, M_2 = \frac{AE}{K_{12}}, M_3 = \frac{EI}{LK_{22}}, M_4 = \frac{EI}{L^2K_{21}}$$

The boundary conditions as defined above and normal functions along with equation (15) result in the system characteristic equation as:

$$|\psi| = 0 \tag{16}$$

where ψ is a 12x12 matrix.

This characteristic equation in determinant form expressed above is a function of relative crack location (γ), local stiffness matrix (K), natural circular frequency (ω) and relative crack depth (φ).

3. EXPERIMENTAL SETUP

A rectangular cross-sectional beam of dimension 1000mm x 50mm x 8 mm prepared for the purpose were put to test to study its vibration characteristics. A vibration testing machine (pulse lite 3560-L machine) was used to study the changes in mode shapes and natural frequency of the beam subjected to free vibration with and without a crack. Specific experiments were conducted step by step with varying locations and crack depths in a systematic manner. As a part of experimental procedure, the specimens were placed in a test rig (Figure 3) and tests were conducted systematically considering different parameters like crack locations, and crack depths. The initial excitation was given on the mid span of the beam using a specialized hammer. To register the 1st, 2nd and 3rd modes of vibration, a piezoelectric accelerometer was placed along the length of beam. The signals representing natural frequency and mode shapes were captured in a vibration analyzer consisting of frequency response spectrum, printer and a desk top computer with dual channel analyzer.

Figure 3. Experimental set up

4. RESULTS AND DISCUSSIONS FROM NUMERICAL AND EXPERIMENTAL ANALYSIS

First three modal data, i.e. natural frequencies and mode shapes are recorded during the conduct of the test. First three natural frequencies are then calculated for each crack location and crack depth using the test specimens. The experimental results obtained from the test are then validated with the corresponding numerical results to establish the integrity of the experimental analysis. Table 1 to Table 5 represent the first three natural frequencies data for various crack positions at different crack depths for a Free-Free beam. It is evident from the experimental data that with increasing crack locations and increasing relative crack depths, the relative natural frequencies are in a decreasing trend. This is due to fact that stiffness decreases for a higher crack depth at a given crack location.

Table 1. Relative natural frequencies for fixed relative crack location=0.15 under various relative crack depths

	crack location(relative)=0.15		
Relative crack depth	**Relative natural frequency (first)**	**Relative natural frequency (second)**	**Relative natural frequency (third)**
0.05	0.96427	0.97409	0.95994
0.15	0.96204	0.97248	0.95744
0.25	0.95982	0.970873	0.95495
0.35	0.95759	0.96925	0.95245
0.45	0.95537	0.96764	0.94996
0.55	0.95314	0.96603	0.94746

Table 2. Relative natural frequencies for fixed relative crack location=0.25 under various relative crack depths

	crack location(relative)=0.25		
Relative crack depth	**Relative natural frequency (first)**	**Relative natural frequency (second)**	**Relative natural frequency (third)**
0.05	0.98238	0.93647	0.93146
0.15	0.98128	0.93251	0.92720
0.25	0.98018	0.92856	0.92293
0.35	0.97909	0.92460	0.91866
0.45	0.97799	0.92065	0.91439
0.55	0.97689	0.91669	0.91012

Table 3. Relative natural frequencies for fixed relative crack location=0.35 under various relative crack depths

	crack location(relative)=0.35		
Relative crack depth	**Relative natural frequency (first)**	**Relative natural frequency (second)**	**Relative natural frequency (third)**
0.05	0.96076	0.93628	0.97909
0.15	0.95795	0.93232	0.97779
0.25	0.95549	0.92835	0.97649
0.35	0.95330	0.92438	0.97518
0.45	0.95056	0.92041	0.97388
0.55	0.94809	0.91644	0.97258

Table 4. Relative natural frequencies for fixed relative crack location=0.45 under various relative crack depths

	crack location(relative)=0.45		
Relative crack depth	**Relative natural frequency (first)**	**Relative natural frequency (second)**	**Relative natural frequency (third)**
0.05	0.93660	0.95338	0.93502
0.15	0.93265	0.95048	0.93097
0.25	0.92869	0.94758	0.92692
0.35	0.924750	0.94468	0.92287
0.45	0.92080	0.94177	0.91883
0.55	0.916856	0.93887	0.91478

Table 5. Relative natural frequencies for fixed relative crack location=0.55 under various relative crack depths

	crack location(relative)=0.55		
Relative crack depth	**Relative natural frequency (first)**	**Relative natural frequency (second)**	**Relative natural frequency (third)**
0.05	0.93642	0.95151	0.93596
0.15	0.92959	0.94849	0.93197
0.25	0.92546	0.94547	0.92798
0.35	0.92133	0.94245	0.92399
0.45	0.91720	0.93943	0.92000
0.55	0.91308	0.93641	0.91601

Figure 4 to Figure 6 represent the graphical comparison of mode shapes obtained from numerical and experimental analysis.

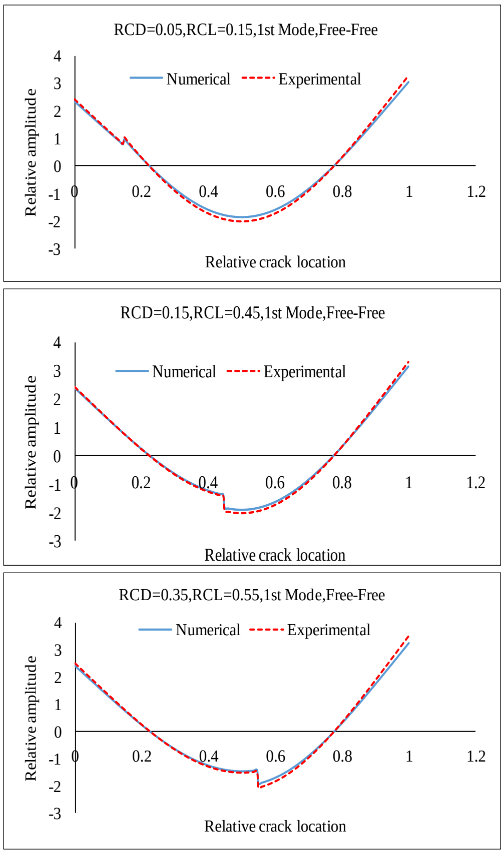

Figure 4. 1st mode of vibration for free-free beam with (a) rcd=0.05, rcl=0.15 (b) rcd=0.15, rcl=0.45 (c) rcd=0.35, rcl=0.55

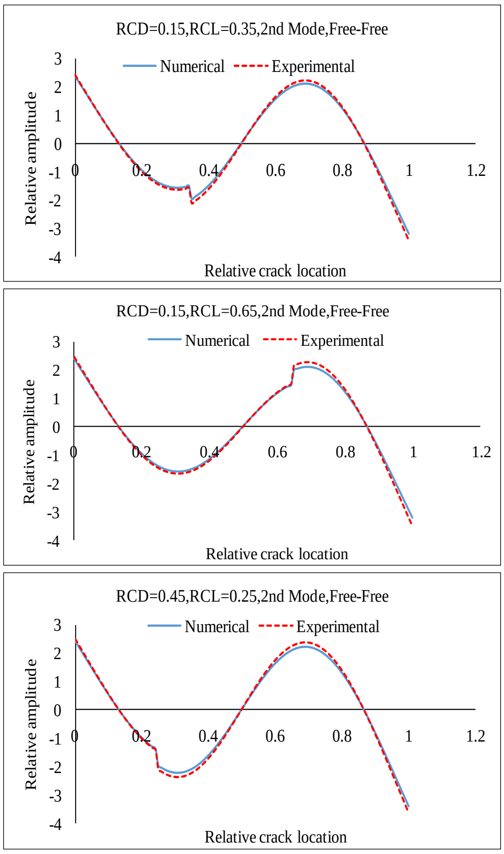

Figure 5. 2nd mode of vibration for free-free beam with (a) rcd=0.15, rcl=0.35 (b) rcd=0.15, rcl=0.65 (c) rcd=0.45, rcl=0.25

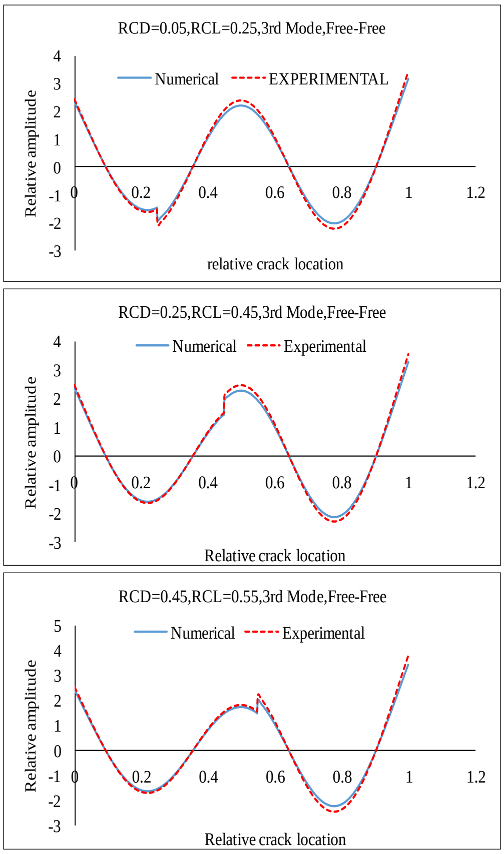

Figure 6. 3rd mode of vibration for free-free beam with (a) rcd=0.05, rcl=0.25 (b) rcd=0.25, rcl=0.45 (c) rcd=0.45, rcl=0.55

5. FUZZY LOGIC

Presence of crack in a structure pose a threat to its life. So, it is highly essential to detect any internal damage occurred due to fatigue of materials. So many researchers have focused their study to find different techniques to identify the cracks in a damaged structure and to estimate the damage severity. The purpose is to either prevent any further damage to the structure or to find the ways to prevent any initiation of cracks in the structure. For this, researchers have proposed many methods like dye penetration, use of sensors, etc. But these conventional methodologies are associated with limitations. In the present study, fuzzy logic as one of the intelligent hybrid technique has been used for crack diagnosis in a vibrating beam structure.

5.1 Fuzzy sets and membership functions

A fuzzy set is fully characterized by its membership functions. Since it is an acceptable fact that most fuzzy sets have a universe of discourse X consisting of the real lines defined by set R. It is nearly an impossible fact to list all the pair of lines that would define the membership function. So the simplest way to define a membership function is to express it mathematically.

5.2 Modelling of fuzzy membership functions

Determination of the fuzzy membership functions play a key role in the design and development of a fuzzy inference system. The chosen membership function decides its fuzzy set. Though membership functions can be formulated into any shapes but few most frequently used membership functions for real applications are trapezoidal, triangular and Gaussian membership functions. Fuzzy set defines degree of membership functions. A non-zero membership value associated with element are considered as support and with a membership value of degree one are considered as core of the fuzzy set. The degree or magnitude of membership function is defined by values ranging from 0 to 1 which is expressed as the height of membership function as shown in Figure 7. Hence, any element that belongs to fuzzy set is defined by a set [0,1].

5.3 Fuzzy inference system

Fuzzy controller uses directly all the fuzzy rules that is considered as the most important application in fuzzy theory. Fuzzy controller consisting of processes called fuzzy inference process and is represented pictorially in Figure 8.

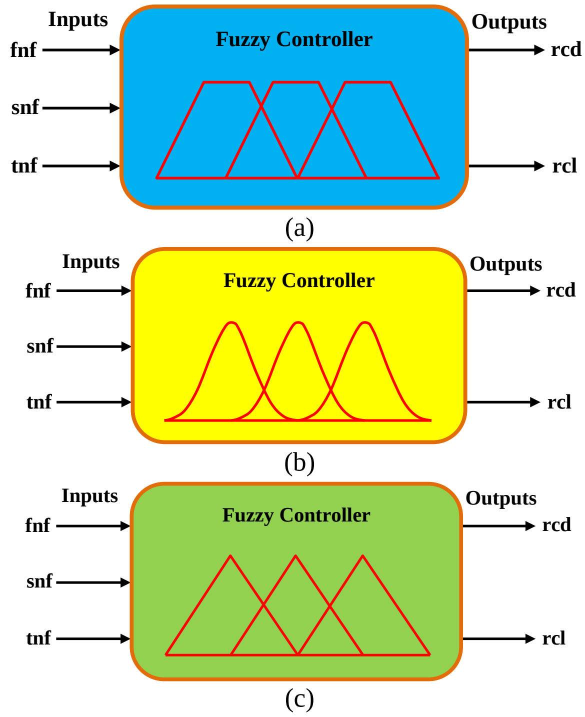

Figure 7. (a) Trapezoidal fuzzy controller (b) Gaussian fuzzy controller (c) Triangular fuzzy controller

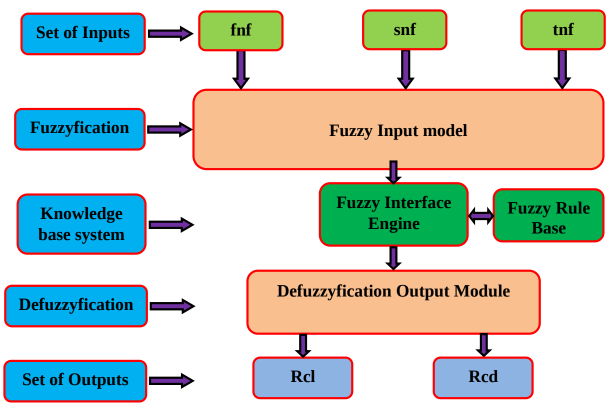

Figure 8. Flow diagram of fuzzy inference system

Fuzzification is the translation of input into truth values and rule evaluation is the process of computing output truth values. Defuzzification is transferring truth values into output (crisp output or actual result). Fuzzy controller or fuzzy logic system gives a scalar output by mapping input data (nonlinear) to output data. The possible mapping of input and output data is done through input-output membership functions. FLS or controller maps data in the form of crisp input and crisp output. The FLS is viewed as complete system when the fuzzy rules are completely defined. A complete fuzzy system uses the independent input parameter and then processed under fuzzy rules and fuzzy linguistics variables give rise to output results. The working of fuzzy system can be broadly classified as following five steps

Step 1: Input to the fuzzy logic system

The input data created is given to the fuzzy inference system and the membership function plays an important role to verify and recognize the extent to which degree, the system is associated to the fuzzy set.

Step 2: Application of fuzzy operators

The proposed fuzzy model after fuzzification checks the establishment of the degree to which its antecedents satisfies to the each of the fuzzy rule data base. A fuzzy operator converts the fuzzy rules with more than one part into one value of the given rule.

Step 3: Application of procedure for fulfilment of fuzzy rules

The output parameters of membership function which is considered as a fuzzy set is reshaped using a function associated to the antecedents.

Step 4: Aggregation of output results

The derived result output from each of fuzzy rule are combined that results into a conclusion from the fuzzy system. The output data is a combined fuzzy set developed through the aggression process.

Step 5: Defuzzification

The fuzzy system converts the output parameter in the form of fuzzy set into crisp form using the methods like centroid, maxima. The result obtained in crisp form is easier for analysis.

Table 6 represents the prediction of best membership function for the current application.

Table 6. Comparison of different membership functions with experimental result for a free-free beam

rfnf	**rsnf**	**rtnf**	Experimental		Triangular Fuzzy Controller		Trapezoidal Fuzzy Controller		Gaussian Fuzzy Controller	
			rcd	**rcl**	**rcd**	**rcl**	**rcd**	**rcl**	**rcd**	**rcl**
0.98187	0.93305	0.92793	0.14718	0.24607	0.14429	0.24338	0.14441	0.24356	0.14467	0.24377
0.95818	0.93311	0.97832	0.14529	0.34796	0.14234	0.34357	0.14249	0.34381	0.14286	0.34394
0.92913	0.94803	0.92738	0.24706	0.44901	0.24427	0.44549	0.24442	0.44553	0.24467	0.44579
0.92278	0.94391	0.92481	0.34391	0.54311	0.34219	0.54220	0.34227	0.54234	0.34248	0.54251
0.91344	0.93667	0.91666	0.54833	0.54858	0.54344	0.54488	0.54359	0.54499	0.54386	0.54528

6. GENETIC ALGORITHM

The workability of the genetic algorithm technique is a Darwin's theory based population survey that contains a chromosome, a gene, a set of population fitness functions, breeding, mutation and selection. The procedure begins with a set of solutions representing chromosomes called as population. The new population are formed from a set of old population on the basis of fitness. Evolution which is motivated by the possibility that the new population are better than the old one. On the basis of fitness criteria, new offspring are generated as a part of new solutions. The above process is repeated until some conditions are attained. The procedure is outlined as below.

Step 1 (start): Random population as chromosomes are selected as input parameters to the problem.

Step 2 (fitness): The fitness of each chromosome as population are then evaluated from the selected population.

Step 3 (new population): The new population are then created by repeating the following steps until the process of creation of new population is complete.

(a) (selection) Parent chromosomes are selected from the population according to their fitness. Better the fitness then more likely to be selected as parent chromosomes.

(b) (cross over) The process of crossover of parent chromosomes create off springs called as children. When no crossover is performed, offspring are regarded as the exact copy of the parent chromosomes.

(c) (mutation) The mutation of offspring create new offspring.

New offspring created are then placed in new population.

Step 4 (replace): The new generated population are then run for the algorithm.

Step 5 (test): The program is then continued to run till the end conditions are satisfied then stop and then return to the best solution in the current population.

Step 6 (loop): Step-2 is repeated.

The crossover and mutation process largely influence the GA's performance.

7. ADAPTIVE RULE BASE TECHNIQUE

This methodology uses a set of assertions that collectively prepare a working memory and a set of rules to specify procedure to act on the assertion set which assist to frame a rule based system. It is a knowledge base system or otherwise called "expert system" consisting of if-then statements. The features of an expert system are on the basis of expertise knowledge available in a specific field that is encoded into a sets of rules.

8. PROPOSED HYBRID CONTROLLER

After formulating the architecture for individual methods, fuzzy logic, genetic algorithm and rule base technique are combined separately to generate hybrid controllers (Figure 9 to Figure 12) and the results obtained from all the controllers are presented in tabular form in Table 7 to Table 10.

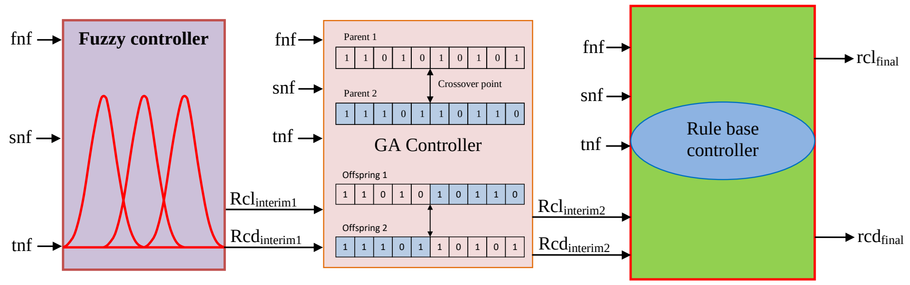

Figure 9. Fuzzy-Genetic-Rule base hybrid controller

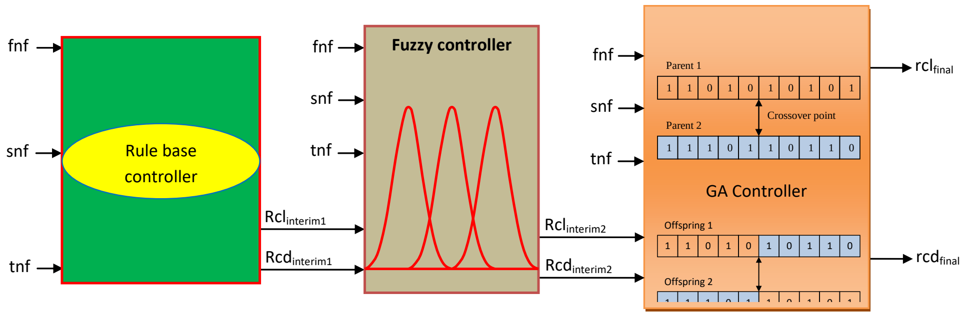

Figure 10. Rule base-Fuzzy-Genetic hybrid controller

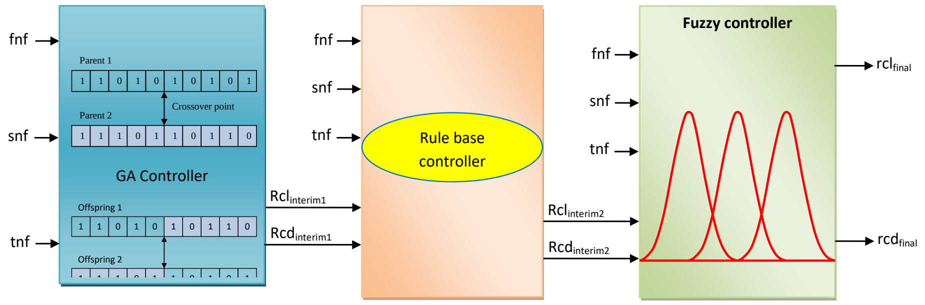

Figure 11. Genetic-Rule base-Fuzzy hybrid controller

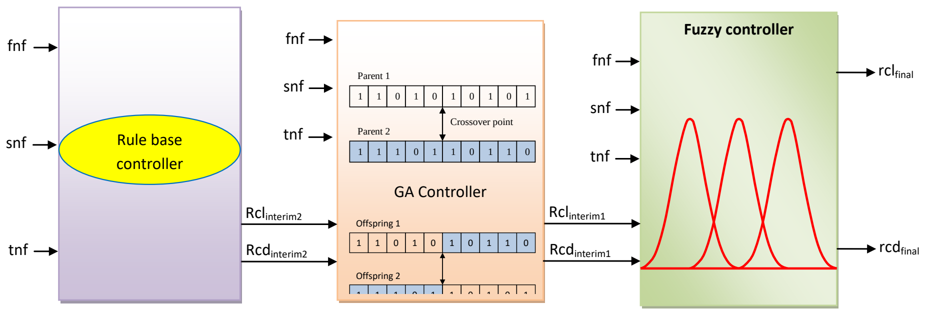

Figure 12. Rule base-Genetic- Fuzzy hybrid controller

Table 7. Comparison of result of hybrid model of Fuzzy logic-genetic algorithm-rule base combinations with that of experimental results

rfnf	rsnf	rtnf	Hybrid Model of Fuzzy, Genetic algorithm and Rule Base model		Experimental result		% Deviation	
			rcd	rcl	rcd	rcl	rcd	rcl
0.98187	0.93305	0.92793	0.14526	0.24488	0.14718	0.24607	1.32	0.48
0.95818	0.93311	0.97832	0.14394	0.34516	0.14529	0.34796	0.93	0.811
0.92913	0.94803	0.92738	0.24519	0.44696	0.24706	0.44901	0.762	0.45
0.92278	0.94391	0.92481	0.34301	0.54246	0.34391	0.54311	0.262	0.119
0.91344	0.93667	0.91666	0.54468	0.54569	0.54833	0.54858	0.670	0.529

Table 8. Comparison of result of hybrid model of Rule base- fuzzy logic -genetic algorithm combinations with that of experimental results

rfnf	rsnf	rtnf	Hybrid Model of Rule Base, Fuzzy and Genetic Algorithm		Experimental result		% deviation	
			rcd	rcl	rcd	rcl	rcd	rcl
0.98187	0.93305	0.92793	0.14664	0.24553	0.14718	0.24607	0.368	0.219
0.95818	0.93311	0.97832	0.14489	0.34739	0.14529	0.34796	0.276	0.164
0.92913	0.94803	0.92738	0.24631	0.44817	0.24706	0.44901	0.304	0.187
0.92278	0.94391	0.92481	0.34339	0.54278	0.34391	0.54311	0.151	0.060
0.91344	0.93667	0.91666	0.54754	0.54768	0.54833	0.54858	0.144	0.045

Table 9. Comparison of result of hybrid model of genetic algorithm -rule base-fuzzy logic - combinations with that of experimental results

rfnf	rsnf	rtnf	Hybrid Model of Genetic Algorithm, Rule Base and Fuzzy model		Experimental result		% Deviation	
			rcd	rcl	rcd	rcl	rcd	rcl
0.98187	0.93305	0.92793	0.14579	0.24498	0.14718	0.24607	0.593	0.444
0.95818	0.93311	0.97832	0.14414	0.34596	0.14529	0.34796	0.797	0.578
0.92913	0.94803	0.92738	0.24613	0.44735	0.24706	0.44901	0.377	0.371
0.92278	0.94391	0.92481	0.34316	0.54269	0.34391	0.54311	0.218	0.077
0.91344	0.93667	0.91666	0.54541	0.54606	0.54833	0.54858	0.535	0.461

Table 10. Comparison of result of hybrid model of rule base-genetic algorithm-fuzzy logic combinations with that of experimental results

rfnf	rsnf	rtnf	Hybrid Model of Rule Base, Genetic Algorithm and Fuzzy model		Experimental result		% Deviation	
			rcd	rcl	rcd	rcl	rcd	rcl
0.98187	0.93305	0.92793	0.14596	0.24508	0.14718	0.24607	0.83	0.40
0.95818	0.93311	0.97832	0.14409	0.34584	0.14529	0.34796	0.008	0.61
0.92913	0.94803	0.92738	0.24549	0.44719	0.24706	0.44901	0.63	0.40
0.92278	0.94391	0.92481	0.34320	0.54264	0.34391	0.54311	0.002	0.086
0.91344	0.93667	0.91666	0.54506	0.54594	0.54833	0.54858	0.59	0.48

9. CONCLUSIONS

The objective of the present research aims at establishing an effective hybrid technique to diagnose cracks in the damaged vibrating beam structure under a complex loading pattern. So a systematic study has been carried out to measure the influence of crack on the vibration characteristics of the beam. Various techniques i.e. numerical, experimental, fuzzy logic, genetic algorithm and rule based hybrid technique have been used to identify the crack location and to understand the performance of the technique for evaluation of the severity of the crack. A detailed study has been performed considering various techniques in hybridized form and its outcome has been compared with the corresponding values of the experimental and numerical result. Based on the performance, the most suitable hybrid technique appropriate to research is chosen and following conclusions have been drawn as below.

1) It may be established here that a local flexibility is induced at the crack position due to crack depth that changes the structural integrity sensitive indicators like relative mode shapes and relative natural frequency.

2) It may be noted that the crack locations and the crack depths influence the natural frequency and mode shape of a vibrating beam. In the present research efforts have been made to locate the position of crack and its severity by adopting hybrid artificial intelligence technique. In such techniques, relative natural frequency obtained from numerical and experimental data are used as inputs to a reverse inference engine controller for predicting the locations and depth of crack in a vibrating beam. Fuzzy logic, Genetic algorithm, adoptive rule based intelligent technique have been used in different combinations.

3) The whole study aims at developing a crack diagnostic tool for crack diagnosis to ascertain crack locations and crack depths in a beam. The influence of vibration parameters like relative mode shapes and relative natural frequencies in presence of cracks have been studied successfully using the developed tool.

4) It may be noted that the Gaussian membership function gives more accurate result as compared to other trapezoidal membership function and triangular membership function as evident from the percentage deviation.

5) The resulted crack locations and crack depths from hybrid intelligent system is in good agreement with the corresponding experimental result and the calculated deviation does not exceed beyond three percent Table 7 to Table 10.

6) The study shows that an increase in crack depth ratio decreases relative natural frequencies due to decrease in stiffness of the beam for given crack location. At higher mode the relative natural frequency is higher due to an

increase in stiffness.

7) It can be established that the Rule Base-Fuzzy-GA hybrid combination has been found to be more accurate and its output as relative crack location and relative crack depth are at close proximate with that of experimental result with minimum deviation.

REFERENCES

[1] Luo W, Shi S, Sun J, Lv Y. (2017). Experimental analysis and numerical simulation on impact response of sand-filled aluminium honeycomb sandwich structure. AMSE Journals-AMSE IIETA publication-2017-Series: Modelling B 86(2): 517-534.

[2] Nan G, Haixin J, Hongliang Z. (2017). The research on flexural behavior experiment of pre-stressed glue-lumber beams after long-term loading. AMSE Journals-AMSE IIETA publication-2017-Series: Modelling B 86(1): 49-62.

[3] Ganguli R. (2001). A fuzzy logic system for ground based structural health monitoring of a helicopter rotor using modal data. Journal of Intelligent Material Systems and Structures 12(6): 397-407.

[4] Sazonov ES, Klinkhachorn P, GangaRao HV, Halabe UB. (2002). Fuzzy logic expert system for automated damage detection from changes in strain energy mode shapes. Nondestructive Testing and Evaluation 18(1): 1-20.

[5] Pawar PM, Ganguli R. (2003). Genetic fuzzy system for damage detection in beams and helicopter rotor blades. Computer Methods in Applied Mechanics and Engineering 192(16-18): 2031-2057.

[6] Chandrashekhar M, Ganguli R. (2009). Uncertainty handling in structural damage detection using fuzzy logic and probabilistic simulation. Mechanical Systems and Signal Processing 23(2): 384-404.

[7] Parhi DR, Kumar DA. (2009). Analysis of methodologies applied for diagnosis of fault in vibrating structures. International Journal of Vehicle Noise and Vibration 5(4): 271-286.

[8] He Y, Guo D, Chu F. (2001). Using genetic algorithms and finite element methods to detect shaft crack for rotor-bearing system. Mathematics and Computers in Simulation 57(1-2): 95-108.

[9] Hao H, Xia Y. (2002). Vibration-based damage detection of structures by genetic algorithm. Journal of Computing in Civil Engineering 16(3): 222-229.

[10] Krawczuk M. (2002) Application of spectral beam finite element with a crack and iterative search technique for damage detection. Finite Elements in Analysis and Design 38(6): 537-548.

[11] He RS, Hwang SF. (2006). Damage detection by an adaptive real-parameter simulated annealing genetic algorithm. Computers & Structures 84(31-32): 2231-2243.

[12] Perera R, Torres R. (2006). Structural damage detection via modal data with genetic algorithms. Journal of Structural Engineering 132(9): 1491-1501.

[13] Panigrahi SK, Chakraverty S, Mishra BK. (2009). Vibration based damage detection in a uniform strength beam using genetic algorithm. Meccanica 44(6): 697.

[14] Pawar PM, Ganguli R. (2005). Matrix crack detection in thin-walled composite beam using genetic fuzzy system. Journal of Intelligent Material Systems and Structures 16(5): 395-409.

[15] Wu Q. (2011). Hybrid fuzzy support vector classifier machine and modified genetic algorithm for automatic car assembly fault diagnosis. Expert Systems with Applications 38(3): 1457-1463.

[16] Lo CH, Chan PT, Wong YK, Rad AB, Cheung KL. (2007). Fuzzy-genetic algorithm for automatic fault detection in HVAC systems. Applied Soft Computing 7(2): 554-560.

[17] Suh MW, Shim MB, Kim MY. (2000). Crack identification using hybrid neuro-genetic technique. Journal of Sound and Vibration 238(4): 617-635.

[18] Saridakis KM, Chasalevris AC, Papadopoulos CA, Dentsoras AJ. (2008). Applying neural networks, genetic algorithms and fuzzy logic for the identification of cracks in shafts by using coupled response measurements. Computers & Structures 86(11-12): 1318-1338.

[19] Kolodziejczyk T, Toscano R, Fouvry S, Morales-Espejel G. (2010). Artificial intelligence as efficient technique for ball bearing fretting wear damage prediction. Wear 68(1-2): 309-315.

[20] Tada H, Paris PC, Irwin GR. (1973). The stress analysis of cracks. Handbook, Del Research Corporation.

NOMENCLATURE

U_i	additional displacement due to bending and axial load
J	strain energy release rate at crack section
a_1	crack depth
α_{ij}	components of local flexibility matrix per unit width
P_1, P_2	axial and bending load respectively
K_{11}, K_{12}	stress intensity factors of mode-I due to load P_1 and P_2 respectively
E	Young's modulus of elasticity of the beam material
σ_i	stress at crack cross section due to axial and bending load
B	width of the beam
L	length of the beam
W	depth of the beam
L_1	location of crack
$U_{1(x\ t)}$, $U_{2(x\ ,t)}$	longitudinal amplitudes along the beam
$Y_{1(x\ t)}$, $Y_{2(x,t)}$	transverse amplitudes across the beam
K_{ij}	local stiffness matrix
A_i	equation constants
$\bar{U}_1, \bar{U}_2$	normal functions defined for the system
M_i	compliance constants
$\bar{Y}_1, \bar{Y}_2$	normal functions defined for the system
F_i	experimentally determined function

Greek symbols

ν	Poisson's ratio
φ	relative crack depth
γ	relative crack location
ω	natural circular frequency
ψ	characteristic equation of the system